Wang *et al. Chem Synth* 2024;4:40
DOI: 10.20517/cs.2024.28

Chemical Synthesis

Supplementary Materials

Post-modified porous aromatic frameworks for carbon dioxide capture

Zihao Wang, Yina Zhang, Li Jiang, Qiance Han, Qihaoyue Wang, Jiangtao Jia*, Guangshan Zhu*

Key Laboratory of Polyoxometalate and Reticular Material Chemistry of Ministry of Education, Faculty of Chemistry, Northeast Normal University, Changchun 130024, Jilin, China.

***Correspondence to:** Prof. Jiangtao Jia, Prof. Guangshan Zhu, Key Laboratory of Polyoxometalate and Reticular Material Chemistry of Ministry of Education, Faculty of Chemistry, Northeast Normal University, 5268 Renmin Street, Changchun 130024, Jilin, China. E-mail: jiangtaojia@nenu.edu.cn; zhugs100@nenu.edu.cn

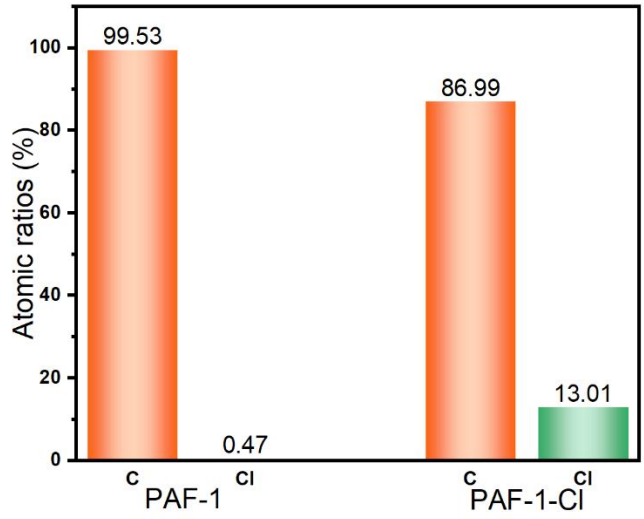

Supplementary Figure 1. Elemental ratios of carbon to chlorine for PAF-1 and PAF-1-Cl from XPS data. The ratios of C/Cl are 0.0047 for PAF-1 and 0.149557 for PAF-1-Cl.

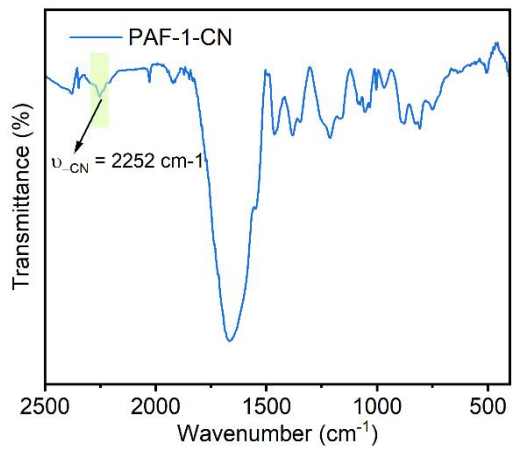

Supplementary Figure 2. FTIR spectra of PAF-1-CN.

Cyanide strictive vibrations occur at 2252 cm^{-1}.

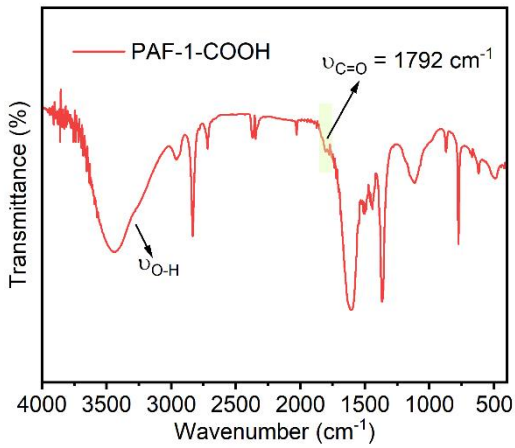

Supplementary Figure 3. FTIR spectra of PAF-1-COOH.

The hydroxyl group stretching vibration is a large broad peak around 3500 cm^{-1} and the carbon-oxygen double bond stretching vibration is at 1792 cm^{-1}.

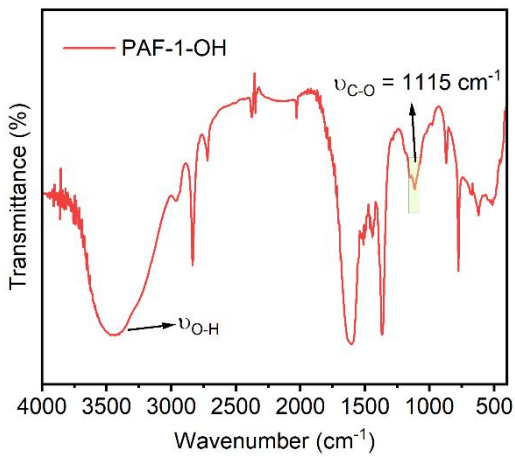

Supplementary Figure 4. FTIR spectra of PAF-1-OH.

The hydroxyl group stretching vibration is a large broad peak around 3500 cm^{-1}.

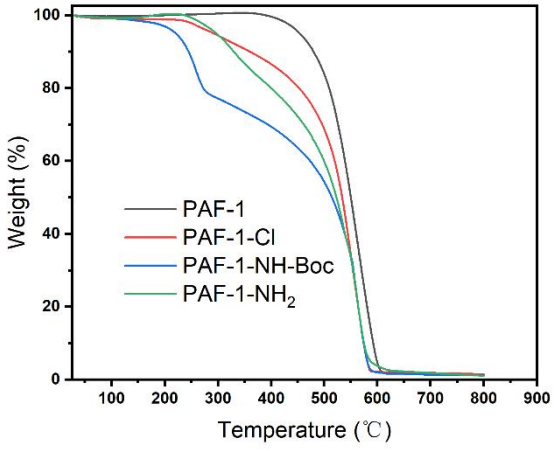

Supplementary Figure 5. TG traces of PAF-1 (black), PAF-1-Cl (red), PAF-1-NH-Boc (blue) and PAF-1-NH_2 (green) under air flow.

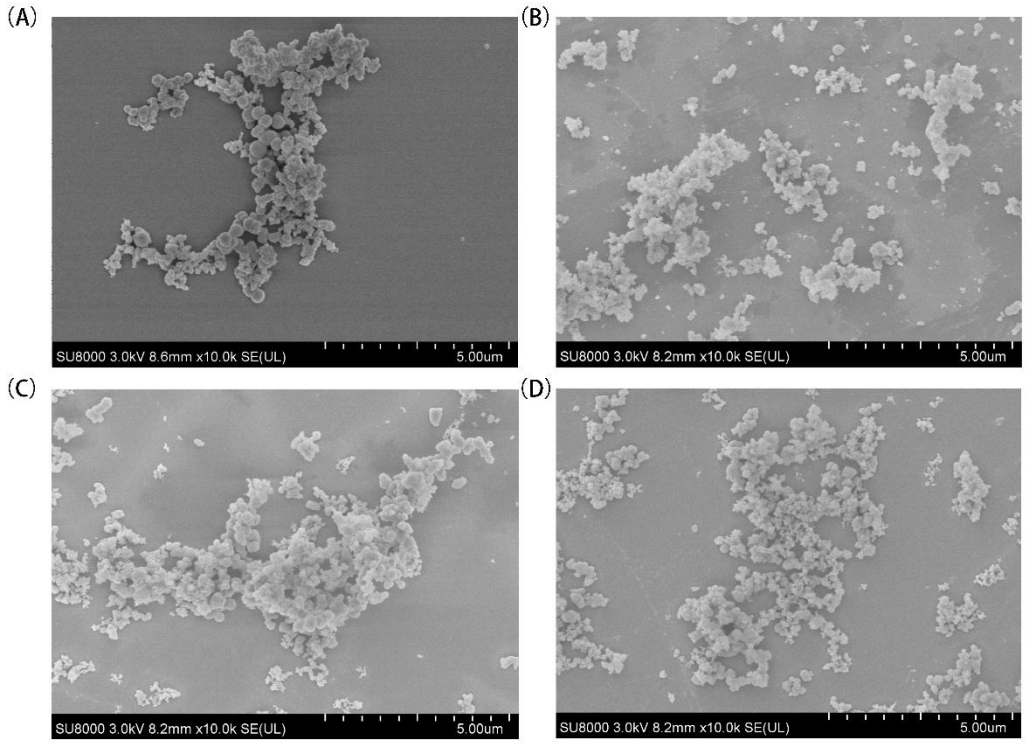

Supplementary Figure 6. Morphology of (A) PAF-1, (B) PAF-1-Cl, (C) PAF-1-NH-Boc and (D) PAF-1-NH_2 by SEM.

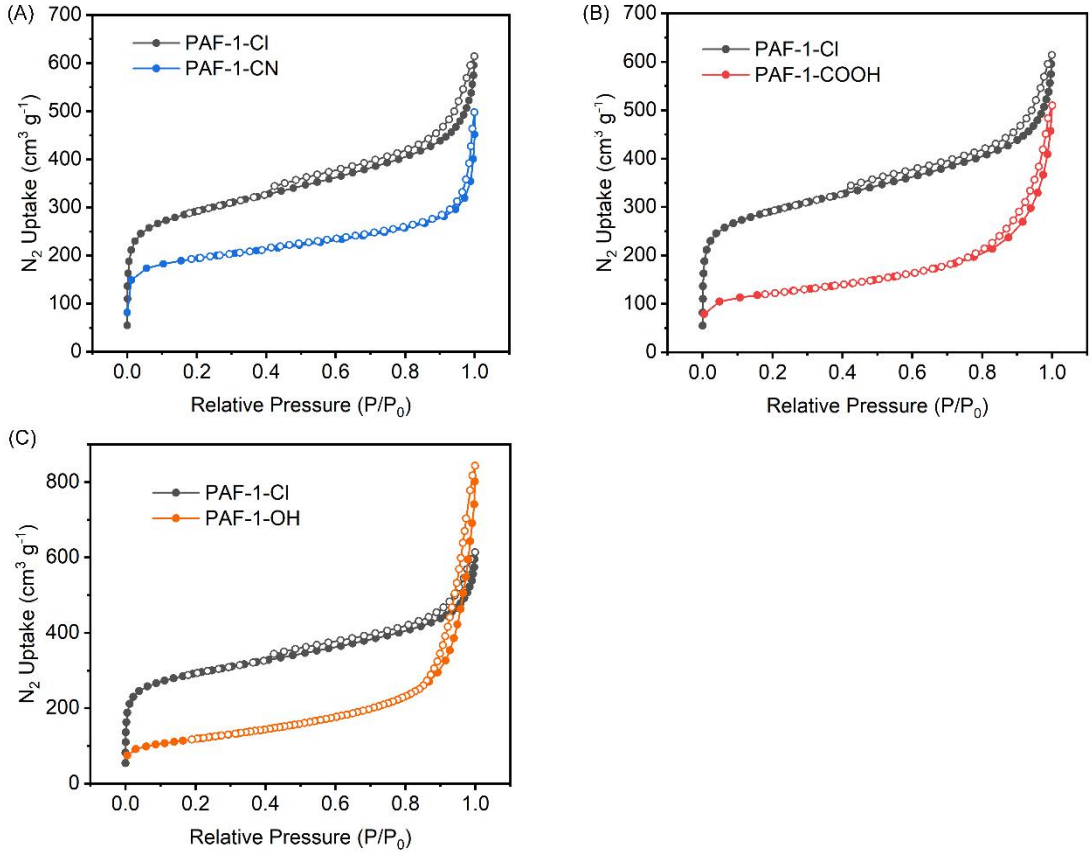

Supplementary Figure 7. The N_2 isotherms of (A) PAF-1-CN, (B) PAF-1-COOH and (C) PAF-1-OH at 77 K.

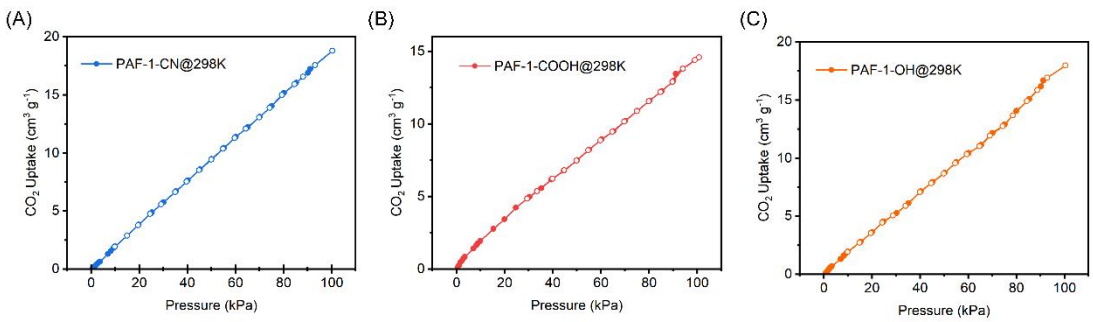

Supplementary Figure 8. The CO_2 isotherms of (A) PAF-1-CN, (B) PAF-1-COOH and (C) PAF-1-OH at 298 K.

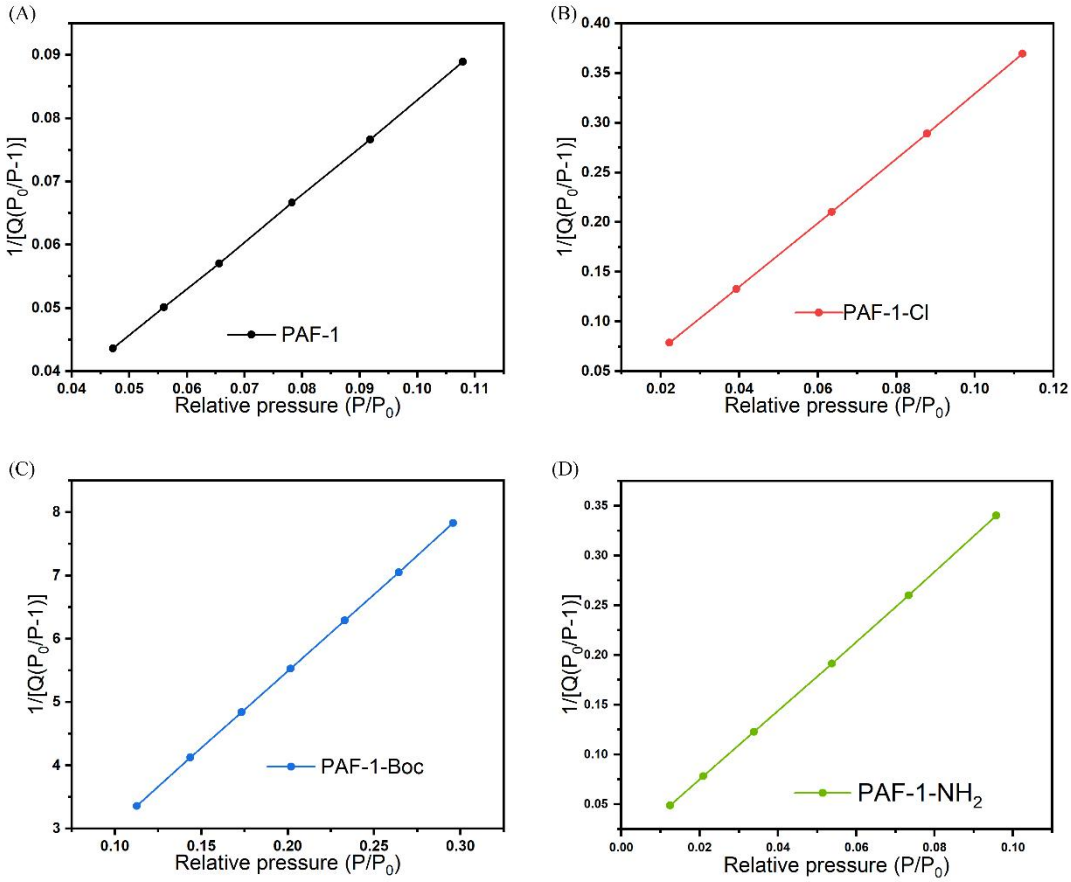

Supplementary Figure 9. Brunauer-Emmett-Teller plot (dots) and linear fitting (line) of N_2 sorption isotherm of PAF-1 BET surface area (A) is 4580 m^2/g with correlation coefficient r=0.999925; PAF-1-Cl BET surface area (B) is 1077 m^2/g with correlation coefficient r=0.999955; PAF-1-NH-Boc BET surface area (C) is 139 m^2/g with correlation coefficient r=0.999991; PAF-1-NH_2 BET surface area (D) is 1002 m^2/g with correlation coefficient r=0.999996.

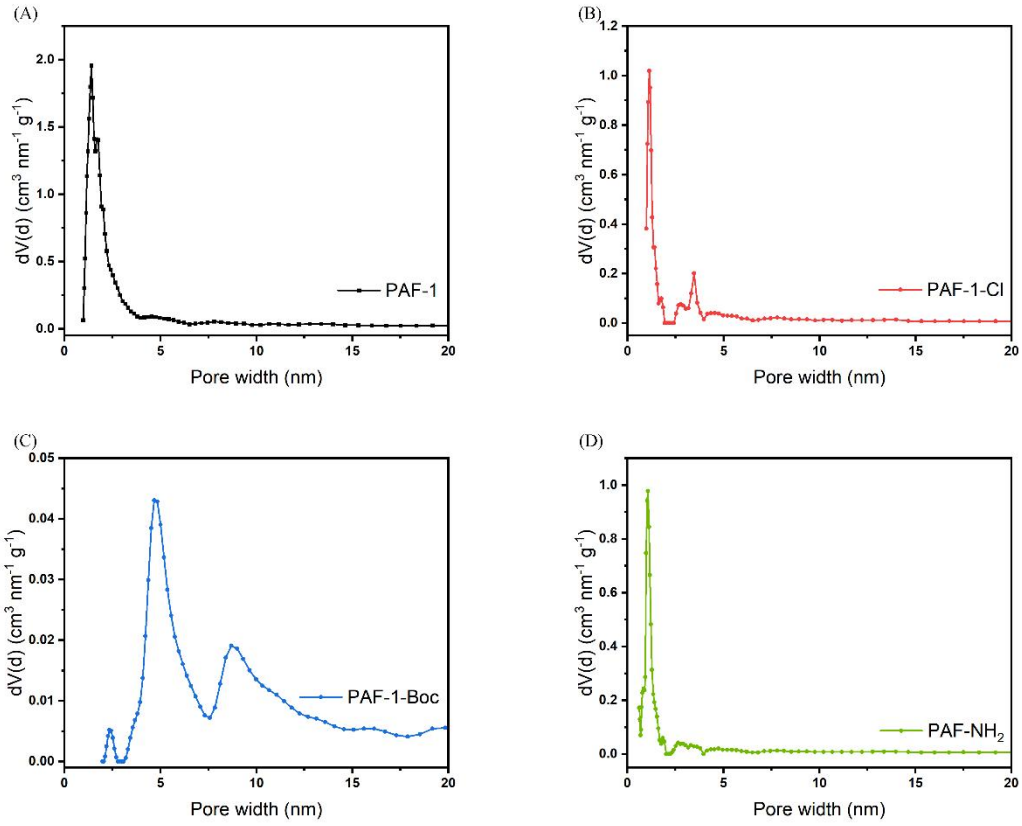

Supplementary Figure 10. The pore size distribution of PAF-1 (A) and its post-modification products (B-D) was determined. Fitting the isotherm based on NLDFT revealed a consistent pore size distribution characterized by a narrow peak at 1.42 nm for PAF-1, 1.18 nm for PAF-1-Cl, minimal perforation for PAF-1-NH-Boc, and 1.08 nm for PAF-1-NH_2.

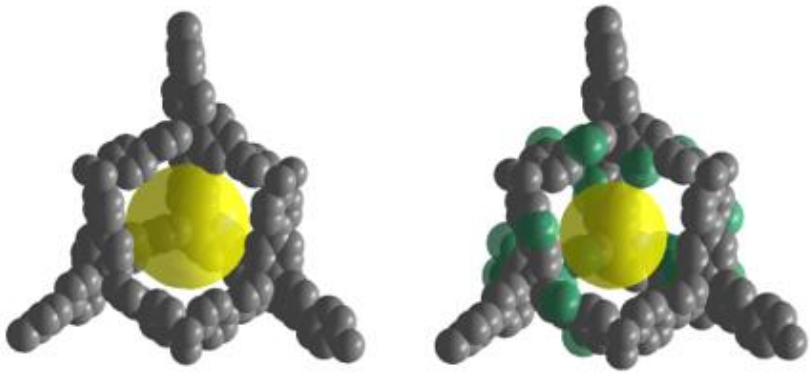

Supplementary Figure 11. The structure of PAF-1 and PAF-1-Cl in CPK style.

After modified by chlorine, the pore volume should decrease. The pore radii of PAF-1 is 7 Å, the Cl and H atom radii are 0.99 Å and 0.37 Å respectively. Therefore, the pore radii after modified could be calculated as followed:

$$r_{PAF-1} = 7\ \text{Å}, r_{PAF-1-Cl} = r_{PAF-1} - 2 * (r_{Cl} - r_H) = 5.76\ \text{Å};$$

And the pore volume should be calculated as equation 1:

$$V_{pore} = \frac{4}{3} \times \pi r^3 \quad (1)$$

i.e. $\frac{V_{PAF-1-Cl}}{V_{PAF-1}} = \frac{r^3_{PAF-1-Cl}}{r^3_{PAF-1}} \approx 55.7\%$

The radius of PAF-1 and PAF-1-Cl are matching the pore size analysis as Supplementary Figure 9 shown. The amount of adsorption was decreased around 45% after modified by -Cl. Meanwhile, as the following image shows, a unit will increase the weight by around 40%. The unit of BET surface area is $m^2 \cdot g^{-1}$, when the building unit was heavier than the PAF-1's, the BET surface area always decreased. Based on the above calculations, the BET surface area of PAF-1-Cl should be calculated as follows:

$$S_{BET-PAF-1-Cl} = S_{BET-PAF-1} \times 55\% \times 40\% = 1007.6\ m^2\ g^{-1}$$

Finally, the calculated BET surface area of PAF-1-Cl is matching the adsorption data.

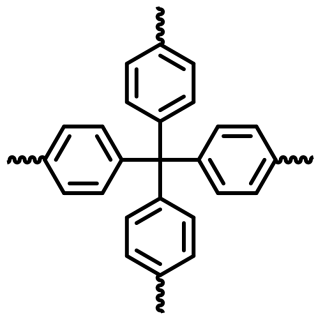

Chemical Formula: C25H16
Molecular Weight: 316.40

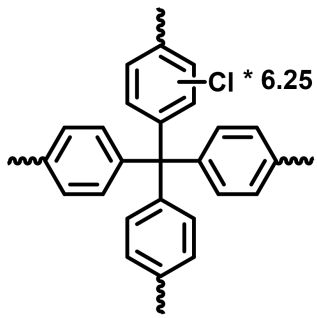

Chemical Formula: $C_{25}H_{9.75}Cl_{6.25}$
Molecular Weight: 531.325

The heat of adsorption is another important parameter for quantitatively assessing the adsorption performance of porous materials for gases. The magnitude of the heat of adsorption determines the affinity of the pore surface for gas molecules, which in turn plays an important role in determining the amount of which in turn plays an important role in determining the energy required for the release of gas molecules during adsorption and desorption.

The common method for calculating the heat of adsorption is the measurement of gas adsorption isotherms at different temperatures.
temperatures and then mathematically fitting them with the virial equation, see equation 2:

$$\ln P = \ln N + \frac{1}{T\sum_{i=0}^{m} a_i N^i} + \sum_{i=0}^{n} b_i N^i \qquad (2)$$

where P is the pressure of the gas (bar), N is the adsorbed amount (mmol·g^{-1}), T is the thermodynamic temperature of the gas (K). a_i and b_i are virial coefficients, and m and n are determined by the number of terms in the equation describing the isotherm. In the case of CO_2 adsorption, the virial equation was firstly used to simultaneously fit the CO_2 adsorption isotherms of the materials at 273 K and 298 K were firstly fitted with the virial equation; then the fitted parameters were used to determine the CO_2 adsorption isotherms of the materials by equation 3:

$$Q_{st} = -R\sum_{i=0}^{m} a_i N^i \qquad (3)$$

Where R is the gas constant (8.314 J·K^{-1}·mol^{-1}).

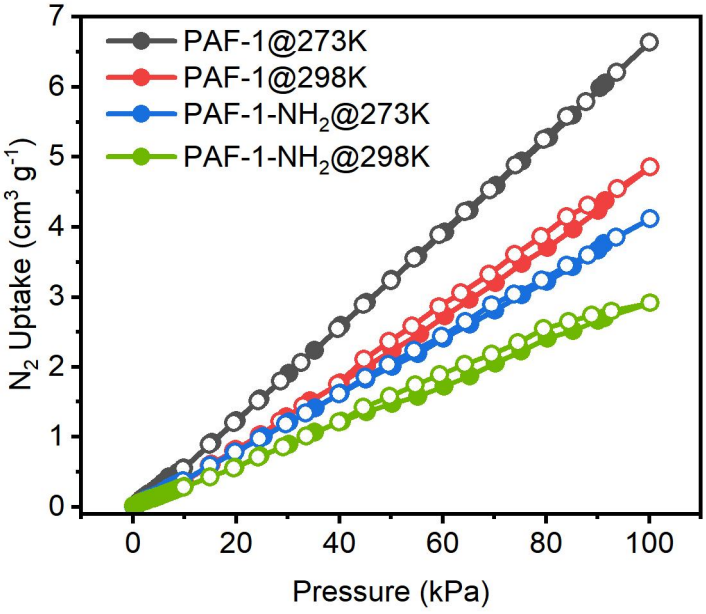

Supplementary Figure 12. The N_2 isotherms of PAF-1 and PAF-1-NH_2 at 273 K and 298 K.

Supplementary Table 1. The CO_2/N_2 selectivity and CO_2 Q_{st} of twelve POPs

POLYMER	CO_2/N_2 selectivity	CO_2 Q_{st} ($kJ \cdot mol^{-1}$)	Ref
PAF-33-NH_2	79.8	32.9	[1]
COF-JLU2	77	31	[2]
BILP-10	57	38.2	[3]
TPILP-1	63	35	[4]
SNW-1	50	35	[5]
TNP-4	27	36.5	[6]
PAF-1-NH_2	163	43	THIS WORK
CMP-1-HN_2	14.6	29.5	[7]
TrzPOP-1	27	29	[8]
TrzPOP-2	72	34	[8]
PPN-6-SO_3NH_4	196	40	[9]
POP-2	155	50	[10]
HCP-MAAMs	104	35	[11]

REFERENCES

1. Yuan R, Ren H, Yan Z, Wang A, Zhu G. Robust tri(4-ethynylphenyl)amine-based porous aromatic frameworks for carbon dioxide capture. *Polym Chem* 2014; 5(7). https://doi.org/10.1039/c3py01252b.

2. Li Z, Zhi Y, Feng X, Ding X, Zou Y, Liu X, et al. An Azine-Linked Covalent Organic Framework: Synthesis, Characterization and Efficient Gas Storage. *Chem Eur J* 2015; 21(34):12079-84. https://doi.org/10.1002/chem.201501206.

3. Rabbani MG, Sekizkardes AK, El-Kadri OM, Kaafarani BR, El-Kaderi HM. Pyrene-directed growth of nanoporous benzimidazole-linked nanofibers and their application to selective CO2 capture and separation. *J Mater Chem A* 2012; 22(48). https://doi.org/10.1039/c2jm34922a.

4. Zhu X, Mahurin SM, An SH, Do-Thanh CL, Tian C, Li Y, et al. Efficient CO(2) capture by a task-specific porous organic polymer bifunctionalized with carbazole and triazine groups. *Chem Commun (Camb)* 2014; 50(59):7933-6. https://doi.org/10.1039/c4cc01588f.

5. Wang C, Li Z, Chen J, Li Z, Yin Y, Cao L, et al. Covalent organic framework modified polyamide nanofiltration membrane with enhanced performance for desalination. *J Membr Sci* 2017; 523:273-81. https://doi.org/10.1016/j.memsci.2016.09.055.

6. Mondal S, Das N. Triptycene based 1,2,3-triazole linked network polymers (TNPs): small gas storage and selective CO2 capture. *J Mater Chem A* 2015; 3(46):23577-86. https://doi.org/10.1039/c5ta06939d.

7. Ratvijitvech T, Dawson R, Laybourn A, Khimyak YZ, Adams DJ, Cooper AI. Post-synthetic modification of conjugated microporous polymers. *Polymers* 2014; 55(1):321-5. https://doi.org/10.1016/j.polymer.2013.06.004.

8. Das SK, Bhanja P, Kundu SK, Mondal S, Bhaumik A. Role of Surface Phenolic-OH Groups in N-Rich Porous Organic Polymers for Enhancing the CO(2) Uptake and CO(2)/N(2) Selectivity: Experimental and Computational Studies. *ACS Appl Mater Interfaces* 2018; 10(28):23813-24. https://doi.org/10.1021/acsami.8b05849.

9. Lu W, Verdegaal WM, Yu J, Balbuena PB, Jeong H-K, Zhou H-C. Building multiple adsorption sites in porous polymer networks for carbon capture applications. *Energy Environ Sci* 2013; 6(12). https://doi.org/10.1039/c3ee42226g.

10. Guillerm V, Weselinski LJ, Alkordi M, Mohideen MI, Belmabkhout Y, Cairns AJ,

et al. Porous organic polymers with anchored aldehydes: a new platform for post-synthetic amine functionalization en route for enhanced CO2 adsorption properties. *Chem Commun (Camb)* 2014; 50(16):1937-40. https://doi.org/10.1039/c3cc48228f.
11. Fayemiwo KA, Vladisavljević GT, Nabavi SA, Benyahia B, Hanak DP, Loponov KN, et al. Nitrogen-rich hyper-crosslinked polymers for low-pressure CO2 capture. *Chem Eng J* 2018; 334:2004-13. https://doi.org/10.1016/j.cej.2017.11.106.